Blocking PPARγ interaction facilitates Nur77 interdiction of fatty acid uptake and suppresses breast cancer progression

Peng-bo Yang[a,1], Pei-pei Hou[a,1], Fu-yuan Liu[a,1], Wen-bin Hong[a,1], Hang-zi Chen[a,1], Xiao-yu Sun[a], Peng Li[a], Yi Zhang[a], Cui-yu Ju[a], Li-juan Luo[a], Sheng-fu Wu[a], Jia-xin Zhou[a], Zhi-jing Wang[a], Jian-ping He[a], Li Li[a], Tong-Jin Zhao[a], Xianming Deng[a], Tianwei Lin[a,2], and Qiao Wu[a,2]

[a]State Key Laboratory of Cellular Stress Biology, State-Province Joint Engineering Laboratory of Targeted Drugs from Natural Products, School of Life Sciences, Xiamen University, 361005 Xiamen, Fujian Province, China

Edited by Tak W. Mak, University of Toronto, Toronto, ON, Canada, and approved September 14, 2020 (received for review February 20, 2020)

Nuclear receptor Nur77 participates in multiple metabolic regulations and plays paradoxical roles in tumorigeneses. Herein, we demonstrated that the knockout of Nur77 stimulated mammary tumor development in two mouse models, which would be reversed by a specific reexpression of Nur77 in mammary tissues. Mechanistically, Nur77 interacted and recruited corepressors, the SWI/SNF complex, to the promoters of *CD36* and *FABP4* to suppress their transcriptions, which hampered the fatty acid uptake, leading to the inhibition of cell proliferation. Peroxisome proliferator-activated receptor-γ (PPARγ) played an antagonistic role in this process through binding to Nur77 to facilitate ubiquitin ligase Trim13-mediated ubiquitination and degradation of Nur77. Cocrystallographic and functional analysis revealed that Csn-B, a Nur77-targeting compound, promoted the formation of Nur77 homodimer to prevent PPARγ binding by steric hindrance, thereby strengthening the Nur77's inhibitory role in breast cancer. Therefore, our study reveals a regulatory function of Nur77 in breast cancer via impeding fatty acid uptake.

fatty acid uptake | nuclear receptors Nur77 and PPARγ | ubiquitination | breast cancer | cytosporone-B

Breast cancer is the most diagnosed cancer and the leading cause of cancer mortality among women worldwide, affecting about 2.1 million women every year (1). Therapeutic strategies based on cancer subtype have improved the clinical outcome of patients with breast cancer in recent decades, but a vast majority of patients diagnosed with advanced breast cancer are confronted with treatment resistance because of the tumor heterogeneity (2). A better understanding of the mechanisms underlying malignant progression of breast cancer and identifying new therapeutic targets and drugs are of high urgency.

Metabolic reprogramming is a common feature of cancer development. In addition to glycometabolic reprogramming prevailing in cancer cells, lipid metabolic remodeling is another characteristic of tumors. Unlike glucose, lipids are not only important energy sources, but also vital material for biomembrane synthesis (3). Therefore, lipid metabolic reprogramming in tumors is more complicated and tissue-specific. Disregulation of lipid metabolism often occurs in breast cancer. Key lipogenic enzymes, including fatty acid synthase (FASN), acetyl-CoA carboxylase (ACC), and ATP citrate lyase, are up-regulated in breast cancer and have been shown to support tumor development (4). For example, the elevated levels of FASN often correlate with poor prognosis in breast cancer patients, and the inhibition of FASN leads to decreased cell viability and tumor growth (4). Knockdown of either ACCα or FASN in breast cancer cells decreases palmitic acid synthesis and leads to apoptosis (5). Cytoplasmic ATP citrate lyase activation is associated with lipid accumulation and required for cyclin E-mediated breast cancer growth (6). All of these data indicate that lipid anabolism cultivates breast cancer development.

Although many cancer cells can synthesize fatty acids de novo, it is not economical to use these fatty acids for energy production and many tumors prefer to directly uptake lipids from the environment to meet the demand. In fact, except the needs for synthesis of cellular lipids and fatty acids, extracellular lipids are a predominant source of energy besides glucose and glutamine in breast cancer (7, 8). Lipids can be transferred from neighboring adipocytes in the mammary tumor microenvironment to breast cancer cells as fuels for tumor growth and aggressiveness, which makes it an attractive treatment strategy to target lipid uptake and transport in breast cancer (9, 10). It is conceivable that the elucidation of the regulatory mechanisms underlying the uptake and transport of exogenous lipids could lead to developing novel and viable strategies to treat breast cancer.

Orphan nuclear receptor Nur77 (also termed TR3 or NGFI-B), a transcription factor encoded by the immediate-early gene *Nr4a1*, belongs to the nuclear receptor superfamily of thyroid, steroid, and retinoic acid (11) and plays distinct roles in different types of cancer. Nur77 is considered to be a pro-oncogenic regulator because of its involvement in the promotion of melanoma cell proliferation through protecting TPβ from oxidation in the mitochondria (12). Nevertheless, Nur77 also has a strong

Significance

It is still a great challenge to identify novel therapeutic strategies for breast cancer, especially for those with treatment resistance. It was demonstrated here that nuclear receptor Nur77 was an effective drug target for breast cancer and compound Csn-B was clinically relevant by binding to Nur77 to prevent peroxisome proliferator-activated receptor-γ (PPARγ) targeting by steric hindrance, thereby inhibiting fatty acid uptake in cells and mouse models. Clinical sample analysis further supported the opposing roles of Nur77 and PPARγ in the patient prognosis of breast cancer. This study not only reveals a inhibitory function of Nur77 on fatty acid uptake for impeding tumor growth, but also identifies Csn-B as an effective therapeutic lead compound for breast cancer.

T.L. and Q.W. conceived the study, made the hypotheses, and designed the experiments; P.Y., P.H., F.L., H.C., X.S., P.L., Y.Z., C.J., L.L., S.W., J.Z., Z.W., and J.H. performed cell and animal experiments and analyzed data; W.H. performed structure analysis; L.L. performed fluorescence quenching assay; T.-J.Z. and X.D. contributed to the discussion of the project; Q.W. supervised the project; and T.L. and Q.W. wrote the paper.

The authors declare no competing interest.

This article is a PNAS Direct Submission.

[1]P.Y., P.H., F.L., W.H., and H.C. contributed equally to this work.

[2]To whom correspondence may be addressed. Email: twlin@xmu.edu.cn or qiaow@xmu.edu.cn.

This article contains supporting information online at https://www.pnas.org/lookup/suppl/doi:10.1073/pnas.2002997117/-/DCSupplemental.

First published October 21, 2020.

tumor-suppressive function. Knockout of Nur77 in mice promotes hepatocarcinogenesis, intestinal tumorigenesis, and development of acute myeloid leukemia (13–15). Although different or even paradoxical regulatory mechanisms and functions of Nur77 in breast cancer have been reported based on cell experiments or xenograft tumors in nude mice (16–21), the role of Nur77 in vivo in breast cancer development remains unknown.

In the presentent study, we demonstrate that Nur77 suppresses breast cancer development in two different mouse tumor models by blocking lipid uptake through transcriptional inhibition of *CD36* and *FABP4*. This role of Nur77, however, is stifled in breast cancer due to peroxisome proliferator-activated receptor-γ (PPARγ)-mediated Nur77 degradation via ubiquitin ligase (E3) Trim13-targeted ubiquitination. Csn-B, the first naturally occurring agonist for Nur77 identified by our group (22), antagonizes PPARγ-mediated degradation of Nur77 through potentiating Nur77 dimerization and impeding the Nur77–PPARγ interaction, which restrains lipid uptake and leads to an aversion of breast cancer progression in a Nur77-dependent manner. Together, these findings not only reveal a suppressive role of Nur77 in breast cancer progression by regulating lipid metabolic pathway, but also identify Csn-B, a Nur77-specific agonist, as an effective therapeutic compound for breast cancer.

Results

Nur77 Plays a Suppressive Role in Breast Cancer Progression. The mouse mammary tumor virus (MMTV)-PyMT transgenic mouse, which carries the polyoma virus middle T antigen with the MMTV promoter, mirrors the multistep progression of human breast cancer beginning from hyperplastic lesions to high-grade carcinomas (23). To identify the potential role of Nur77 in mammary tumor progression, MMTV-PyMT mice were crossed with either WT or Nur77 knockout (Nur77-KO) mice to generate PyMT-WT and PyMT-KO mice. PyMT mRNA levels in primary tumors of both PyMT-WT and PyMT-KO groups were comparable (*SI Appendix*, Fig. S1*A*), precluding the influence of Nur77 on the expression of PyMT. In PyMT-WT mice, the first palpable tumors occurred at the age of 47 d old, while 50% of them developed tumors at the age of about 64 d old. In PyMT-KO mice, the first palpable tumors appeared at the age of 35 d, and 50% of the mice developed tumors at the age of about 43 d old, earlier than PyMT-WT mice (Fig. 1 *A*, *Upper*). At the age of 84 d old, the average mammary tumor weight was 0.663 g in PyMT-WT mice but 3.408 g in PyMT-KO mice (Fig. 1 *A*, *Lower*). At the age of 8 wk old, breast glands from PyMT-WT mice displayed features of hyperplastic lesion with clusters of densely packed lobules formed on the duct with portions of normal ductal structures retained. The breast glands from PyMT-KO mice, however, developed adenoma/mammary intraepithelial neoplasia with numerous and larger lesions and intraluminal proliferation at the age of 10 wk old. At this stage, PyMT-KO breast glands progressed to poorly differentiated carcinomas, which would not be observed in PyMT-WT mice until the age of 12 wk old or older (*SI Appendix*, Fig. S1*B*). In parallel, the Nur77 expression decreased progressively during breast cancer tumorigenesis, both in mammary tissue and isolated primary mammary epithelial/tumor cells from PyMT-WT mice (Fig. 1*B* and *SI Appendix*, Fig. S1*C*).

The inhibitory effect of Nur77 on mammary tumor was also corroborated in chemical carcinogen-induced tumorigenesis. Combinational treatment of medroxyprogesterone acetate (MPA) and 7, 12-dimethylbenzanthracene (DMBA) induces formation of mammary tumors with histological characteristics of adenocarcinoma, adenosquamous carcinoma, and adenomyoepithelioma carcinoma (24). While virtually all Nur77 KO mice developed mammary tumors at the age of 91 d old, 32% of WT mice were free of tumors (Fig. 1 *C*, *Upper*). Mammary tumor progression was obviously facilitated (*SI Appendix*, Fig. S1*D*), and the tumor weight was greatly increased in Nur77-KO mice as compare to WT mice (Fig. 1 *C*, *Lower*). Similarly, tumor samples and primary mammary epithelial/tumor cells from these MPA/DMBA-treated WT mice were with reduced Nur77 expression during tumor progression (Fig. 1*D* and *SI Appendix*, Fig. S1*E*). These results indicate a negative correlation between Nur77 expression and breast cancer development in vivo.

Nur77 is widely expressed in mouse mammary gland (Fig. 1 *B* and *D*). To further substantiate the Nur77 suppressive role in mammary epithelium, we generated a ROSA26$^{\text{loxp-stop-loxp-Nur77}}$ transgenic mice (LSL-Nur77) based on the Nur77-KO background (*SI Appendix*, Fig. S1*F*). When crossed with MMTV-Cre mice, the specific reexpression of Nur77 in mammary epithelial cells in Nur77-KO mice was clearly observed (*SI Appendix*, Fig. S1*G*). LSL-Nur77 mice were then crossed with PyMT-KO;MMTV-Cre mice several times to generate PyMT-KO;LSL-Nur77 and PyMT-KO;LSL-Nur77;MMTV-Cre mice (*SI Appendix*, Fig. S1*F*). The onset of tumor in PyMT-KO;LSL-Nur77;MMTV-Cre mice trailed significantly behind PyMT-KO;LSL-Nur77 mice (Fig. 1 *E*, *Upper*). As expected, tumorigenesis was inhibited, and tumor sizes and weights were reduced in PyMT-KO;LSL-Nur77;MMTV-Cre mice as compared to PyMT-KO;LSL-Nur77 mice (Fig. 1 *E*, *Lower*). Again, with the progression of mammary tumors (*SI Appendix*, Fig. S1*H*), the expression of Nur77 was gradually decreased in mammary tissue and isolated primary mammary epithelial/tumor cells from PyMT-KO;LSL-Nur77;MMTV-Cre mice (Fig. 1*F* and *SI Appendix*, Fig. S1*I*). All of these data strongly support the notion that Nur77 plays a suppressive role in breast cancer progression.

Nur77 Blocks Fatty Acid Uptake to Inhibit the Proliferation of Breast Cancer Cells. The expression levels of Ki67, a marker for cell proliferation, in tumors of either PyMT-KO or MPA/DMBA-treated KO mice were significantly elevated as compared to the corresponding WT mice. In contrast, the expression of Ki67 was decreased in tumors of PyMT-KO;LSL-Nur77;MMTV-Cre mice (Fig. 2*A*). These results inferred a suppressive role for Nur77 in the expansion of mammary epithelial cells and subsequent tumorigenesis. The mammary microenvironment consists of adipocytes and adipocyte precursors. Adipocytes, as an external lipid donor, provide energydense lipids to breast cancer cells to support their rapid growth (10). It could be shown that the tumor periphery adjacent to adipose tissue was predominantly consisted of Ki67 expressing cells, but the tumor cores were essentially devoid of Ki67 staining (Fig. 2*A*). These data suggested that the adipocytes might be an important source of materials for the proliferation of mammary tumor cells in a process regulated by Nur77, which was corroborated by several evidences. First, there were more abundant lipid droplets in Ki67 expressing cells in PyMT-KO tumor sample than in PyMT-WT tumor sample as was detected by Bodipy staining (Fig. 2*B*). Second, when primary cells from PyMT mammary tumors were cocultured with adipocytes isolated from the mouse mammary gland, the cell proliferation for the PyMT-KO primary cells was increased significantly higher than that for the PyMT-WT primary cells (Fig. 2*C*). Similarly, there were more lipid droplets in PyMT-KO primary cells than in PyMT-WT primary cells (Fig. 2*D*), implicating a link between the Nur77-associated arrest of mammary tumor cell growth and the presence of external adipocytes. It could be shown that knockout of Nur77 in primary tumor cells not only increased the intracellular lipid content, but also directly enhanced fatty acid uptake, as revealed by using a green fluorescent or radiolabeled fatty acid (BODIPY FL C16 or [9,10-^{3}H] palmitate acid) (Fig. 2*E*). Third, when a lipid mixture was substituted for adipocytes, PyMT-KO primary cells proliferated significantly better than PyMT-WT primary cells (Fig. 2*F*). Substantially more lipid droplets were accumulated in PyMT-KO primary cells than in PyMT-WT primary cells (Fig. 2 *G* and *H*). No such differences were detected between these two primary cells without either adipocytes or lipid mixture. Finally, the human breast cancer MCF-7 cells behaved similarly to PyMT-KO primary tumor cells in cell proliferation (*SI Appendix*, Fig. S2*A*), lipid droplet accumulation (*SI Appendix*, Fig. S2*B*), and fatty acid uptake

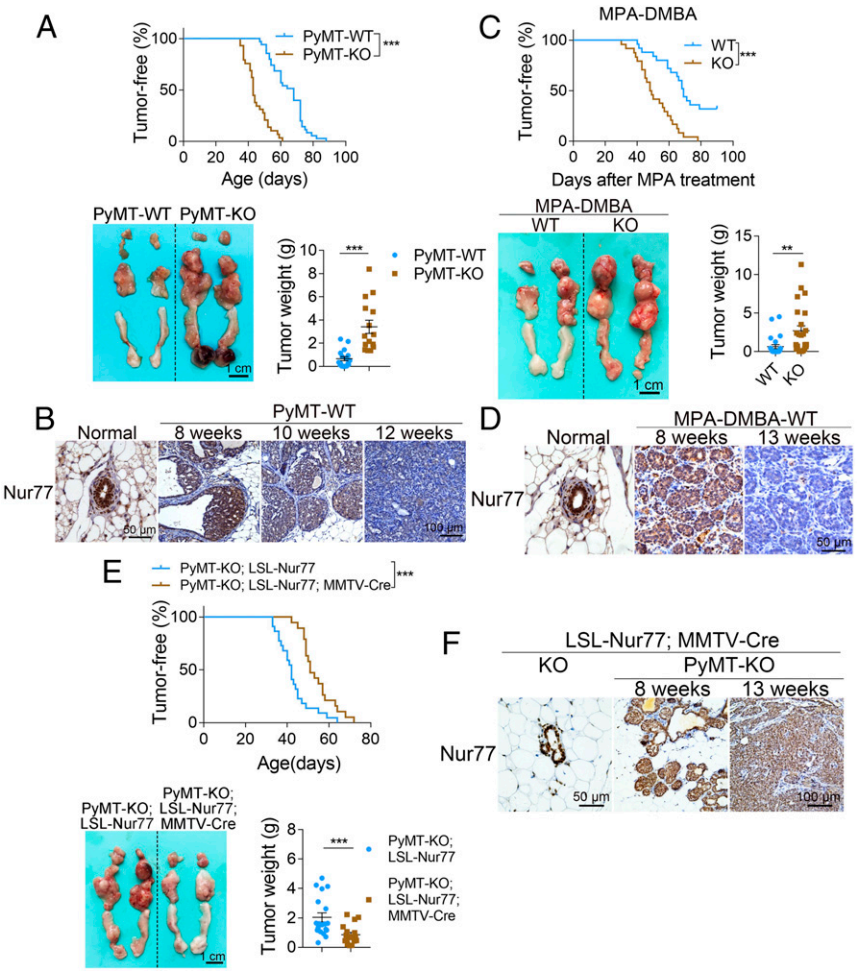

Fig. 1. Nur77 plays an inhibitory effect on breast cancer progression. (*A*, *C*, and *E*, *Upper*), Kaplan–Meier plots for mammary tumor-free survival of WT (n = 35) and Nur77 KO (n = 29) female mice in MMTV-PyMT mouse model (*A*), WT (n = 25) and Nur77 KO (n = 24) female mice in MPA/DMBA mouse model (*C*), or PyMT-KO;LSL-Nur77 (n = 22) and PyMT-KO;LSL-Nur77;MMTV-Cre (n = 19) female mice that reexpressing Nur77 in mammary tissue of Nur77 knockout MMTV-PyMT mouse model (*E*). (*Lower*) Representative images of mammary glands and the total tumor weights in MMTV-PyMT (12 wk; n = 17 for WT, n = 15 for KO), MPA/DMBA (13 wk; n = 25 for WT, n = 24 for KO), and PyMT-KO;LSL-Nur77;MMTV-Cre female mouse models (13 wk; n = 19 for PyMT-KO;LSL-Nur77, n = 18 for PyMT-KO;LSL-Nur77;MMTV-Cre). (*B*, *D*, and *F*) Expression of Nur77 in mammary tissue from normal mice and tumor tissues from the above three mouse models, detected by immunohistochemistry. Data are presented as mean ± SEM $^{**}P < 0.01$, $^{***}P < 0.001$.

(*SI Appendix*, Fig. S2*C*), when its endogenous Nur77 expression was knocked down by shRNA (*SI Appendix*, Fig. S2*D*). Together, these data indicated that the Nur77 deficiency facilitated the uptake of exogenous fatty acids by breast cancer cells for rapid proliferation.

Nur77 Blocks Fatty Acid Absorption by Suppressing CD36 and FABP4 Expression. As Nur77 was mainly expressed in the nucleus of breast cancer MCF-7 cells (*SI Appendix*, Fig. S3*A*), it is possible that Nur77 may function as a transcription factor to control fatty acid uptake. To globally evaluate the influence of Nur77 on gene expression in mammary tumors, primary tumor cells from either PyMT-WT or PyMT-KO tumor samples were collected for RNA sequencing (RNA-seq). Gene set enrichment analysis (GSEA) of RNA-seq data demonstrated that gene signatures for lipids metabolism as well as lipids and organic acids transport were negatively enriched in PyMT-WT primary tumor cells (Fig. 3*A*), suggesting that Nur77 may play an inhibitory role on fatty acid uptake in mammary tumors. Notably, *CD36* and *FABP4*, which have been reported to be involved in cellular uptake and transport of fatty acids (25, 26), were among the most obvious genes down-regulated by Nur77 (Fig. 3*A*). Consistent with the RNA-seq results, knockdown of Nur77 distinctly up-regulated the mRNA levels of CD36 and FABP4 without affecting other members of the FABP family in MCF-7 breast cancer cells (Fig. 3*B*). Knockdown of either CD36 or FABP4 in MCF-7 cells (*SI Appendix*, Fig. S3*B*) decreased fatty acid uptake (*SI Appendix*, Fig. S3*C*). However, if it was a prior knockdown of both CD36 and FABP4 (*SI Appendix*, Fig. S3*D*), a further knockdown of Nur77 resulted in no difference on fatty acid uptake and the lipid content even in the presence of the lipid mixture (Fig. 3*C*). So, the knockdown of both CD36 and FABP4 abolished Nur77's influence on cell proliferation (Fig. 3*D*). It could be concluded that it was through downregulating the expressions of CD36 and FABP4 that Nur77 dampened the fatty acid uptake and breast cancer cell proliferation.

Nur77 down-regulation of CD36 and FABP4 expressions at the mRNA and protein levels was detected in the PyMT primary tumor cells (Fig. 3*E*). Moreover, the negative regulation of Nur77 on CD36 and FABP4 protein expressions were also observed in tumor tissues of PyMT mice (Fig. 3*F*). With the progression of mammary tumors, the expression of CD36 and FABP4 gradually increased in PyMT-WT tumor tissues (Fig. 3*G*), reminiscent of the fact that the Nur77 expression was decreased during tumor progression (Fig. 1*B*). Clearly, Nur77 is upstream of CD36 and FABP4, and the Nur77-associated down-regulation of CD36 and FABP4 expression may well explain its inhibition of cell proliferation through impeding fatty acid uptake from the microenvironment of breast cancer.

Nur77 Recruits SWI/SNF Complex to Down-Regulate CD36/FABP4 Transcription. The mechanism of Nur77 regulation of CD36 and FABP4 gene expression was further investigated. Transfection of Nur77 into MCF-7 cells repressed the transcription activities of CD36 and FABP4 promoters (Fig. 4*A*). Sequence analysis revealed that there were several sequences similar to the response element for Nur77 in the CD36 and FABP4 promoters (*SI Appendix*, Fig. S4*A*). These sequences were designated as NBRE-like (NBRE-L)

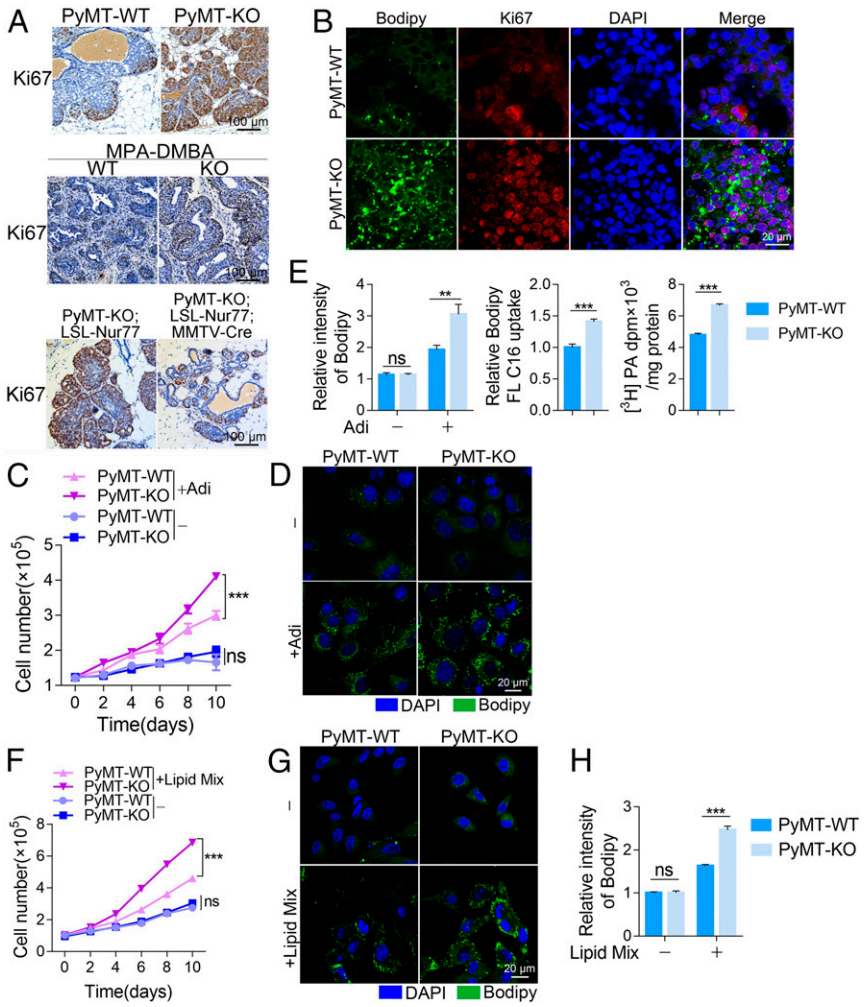

Fig. 2. Blocking lipid uptake by Nur77 contributes to growth inhibition of breast cancer cells. (*A*) Evaluation of the proliferative status by Ki67 IHC staining in mammary tumors from MMTV-PyMT (8 wk), MPA/DMBA (13 wk), and PyMT-KO;LSL-Nur77;MMTV-Cre (13 wk) mouse models. (*B*) Lipid droplets indicated by Bodipy 493/503 in Ki67$^+$ cells. Tumor samples were from PyMT mouse model. (*C*, *D*, *F*, and *G*) Comparison of cell proliferation (*C* and *F*) and lipid-droplet contents (*D* and *G*) in primary mammary tumor cells from WT or Nur77 KO female mice in PyMT mouse model ($n = 3$). Cells were cultured in the medium containing 0.5% lipoprotein-deficient serum (LPDS) with or without adipocyte coculture (*C* and *D*), or lipid mixture addition (*F* and *G*) for the indicated times (*C* and *F*) or 24 h (*D* and *G*). (*E* and *H*) Analysis of lipid content (*E*, *Left*, and *H*) and fatty acid uptake (*E*, *Center* and *Right*) in primary cells from mammary tumors of PyMT mice. Bodipy FL C16 or [9,10-^{3}H] palmitate acid was employed to evaluate fatty acid uptake. Coculture conditions were the same as above. DAPI was used to stain the nucleus. Data are presented as the mean ± SEM of two or three independent experiments. $^{**}P < 0.01$, $^{***}P < 0.001$, ns: not significant.

sequences. Further chromatin immunoprecipitation (ChIP) assays indicated that Nur77 could bind to NBRE-L2, -L3, and -L4 in the CD36 promoter and NBRE-L1 and -L3 in the FABP4 promoter (Fig. 4*B*). Luciferase assays revealed that the deletion of one single NBRE-L element was not sufficient to abolished Nur77 modulation on either CD36 or FABP4 promoter activity. However, when all of the Nur77-interacting elements (i.e., NBRE-L2, -L3, and -L4 in the CD36 promoter or NBRE-L1 and -L3 in the FABP4 promoter) were deleted, Nur77 lost its suppressive activity on these genes (Fig. 4*A* and *SI Appendix*, Fig. S4*A*). Consistently, combined mutation of the NBRE-L2, -L3, and -L4 in the CD36 promoter or NBRE-L1 and -L3 in the FABP4 promoter was sufficient to abrogate the suppressive function of Nur77 on their promoter activity (Fig. 4*C* and *SI Appendix*, Fig. S4*A*). Therefore, it is the Nur77 binding to the promoters of CD36 and FABP4 that leads to the repression of their transcription.

Analysis of Nur77 binding proteins in the nucleus by using mass spectrometry and the STRING database indicated that several transcriptional corepressors, such as the SWI/SNF complex and HDAC1, could be novel binding partners to Nur77 (*SI Appendix*, Fig. S4*B* and Dataset S1). Knockdown of HDAC1 effectively elevated the mRNA levels of CD36 and FABP4 (*SI Appendix*, Fig. S4 *C* and *D*), consistent with the previous finding that HDAC1 was important for the transrepression activity of Nur77 on its downstream genes (27). Among the eight identified SWI/SNF complex subunits, only BRM, BAF170, and BAF155 were shown to significantly influence the gene-expression levels of CD36 and FABP4 (*SI Appendix*, Fig. S4 *C* and *D*). We thus investigated the involvements of BRM, BAF170, BAF155, and HDAC1 in Nur77-mediated repression of CD36 and FABP4. Evidently, Nur77 interacted with BRM, BAF170, BAF155, and HDAC1 in MCF-7 cells (Fig. 4*D*), which was closely associated with the recruitments of these corepressors to the regions around Nur77-binding elements in the CD36 and FABP4 promoters, as revealed by ChIP assays (Fig. 4 *E* and *F*). When Nur77 was knocked down, the associations of these corepressors with CD36 and FABP4 promoters were obviously diminished (Fig. 4 *E* and *F*). Given the histone deacetylation activity of HDAC1, we also tested the histone acetylation level in CD36 and FABP4 promoters and found that the H3K9 and H4K8 acetylation levels in these promoters were substantially suppressed via Nur77 mediation (Fig. 4*G*). As a result, Nur77 substantially suppressed the promoter activities and mRNA levels of CD36 and FABP4; however, knocking down the SWI/SNF subunits or HDAC1 obviously dampened this inhibitory effect of Nur77 (Fig. 4 *H* and *I*). Therefore, it is likely that Nur77 suppresses CD36 and FABP4 expression through the recruitment of the SWI/SNF complex and HDAC1, which is corelated with the suppression of histone acetylation in CD36 and FABP4 promoters (*SI Appendix*, Fig. S4*E*).

PPARγ Interaction Induces Nur77 Degradation by Recruiting Trim13. Analysis by mass spectrometry of Nur77 immunoprecipitates from the nucleus of MCF-7 cells also indicated that nuclear receptor PPARγ, known for its role in regulating lipid metabolism, such as lipid uptake (28, 29), could be a novel Nur77 binding protein (*SI Appendix*, Fig. S4*B* and Dataset S1). PPARγ was also predominant

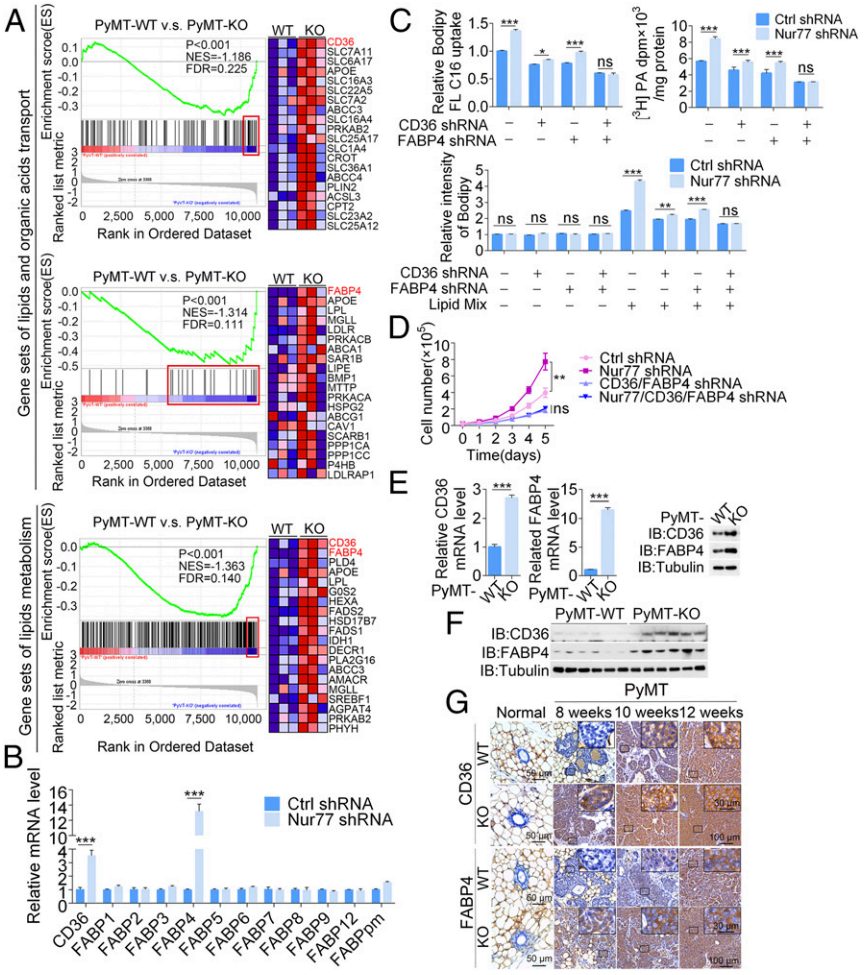

Fig. 3. Nur77 down-regulates CD36 and FABP4 to block fatty acid absorption. (*A*) The expression of genes involved in lipids metabolism. GSEA of lipid and organic acids transport-related (*Upper* and *Middle*) and lipids metabolism-related gene signatures (*Lower*) in PyMT-WT versus PyMT-KO primary tumor cells. Heatmap illustrates the most obvious genes inhibited by Nur77 in each gene set. FDR, false-discovery rate; NES, normalized enrichment score. (*B*) The expression levels of different genes in Nur77 knockdown MCF-7 cells. (*C* and *D*) Detection of fatty acid uptake by Bodipy FL C16 (*C*, *Upper Left*) or [9,10-^{3}H] palmitate acid (*C*, *Upper Right*), lipid droplets accumulation (*C*, *Lower*), and cell proliferation (*D*) in MCF-7 cells. CD36 and FABP4 were separately or simultaneously knocked down as indicated, and Nur77 was then knocked down in the cells. Cells were cultured in medium with lipid mixture (*D*). (*E*) The mRNA (*Left*) and protein (*Right*) levels of CD36 or FABP4 in primary cells from mammary tumors of PyMT mice. (*F* and *G*) The protein expression levels of CD36 and FABP4 in mammary tumor samples of PyMT mice, detected by Western blotting (*F*, $n = 6$) and IHC (*G*). Tubulin was used to determine the loading of total proteins. All data, except *A*, *E* (*Right*), *F*, and *G*, are presented as the mean ± SEM of two or three independent experiments. *$P < 0.05$, **$P < 0.01$, ***$P < 0.001$, ns: not significant.

in the nucleus of MCF-7 cells (*SI Appendix*, Fig. S5*A*). The interaction between PPARγ and Nur77 was confirmed by transfection or endogenous coimmunoprecipitation (co-IP) assays (*SI Appendix*, Fig. S5*B*). PPARγ expression was gradually elevated in mammary tumor tissues during tumor progression (Fig. 5*A*) in a reverse pattern to the Nur77 expression (Fig. 1*B*). It was reported that PPAR family members, such as PPARα and PPARγ, are transcriptional activators of CD36 and FABP4 through interacting with RXR (28, 30); however, the repressive effect of Nur77 on CD36 and FABP4 expression was not through suppressing PPARs. In the present case, PPARγ and PPARα protein levels in primary tumors of PyMT-WT mice were comparable to that in PyMT-KO mice (*SI Appendix*, Fig. S5*C*). In MCF-7 cells, knockdown of Nur77 influenced neither the expression level nor the transcriptional activity of PPARγ (*SI Appendix*, Fig. S5*D*). Moreover, Nur77 could still effectively suppress the mRNA level of CD36 and FABP4 in MCF-7 cells, no matter that PPARγ was knocked down or overexpressed together with its partner RXRα (*SI Appendix*, Fig. S5 *E* and *F*). Clearly, PPARγ did not function as a downstream factor for Nur77 in suppressing CD36 and FABP4.

Although overexpression of PPARγ did not affect Nur77 gene-expression level (*SI Appendix*, Fig. S5*G*), it decreased the endogenous expression level of Nur77 protein in MCF-7 cells (Fig. 5 *B*, *Left*), in contrast to the elevated Nur77 protein level when PPARγ was knocked down (Fig. 5 *B*, *Right*). The transcription activity of PPARγ played no role in modulating the Nur77 expression, as three transcriptionally inactive PPARγ mutants (PPARγ^{C114R}, PPARγ^{C131Y}, PPARγ^{C162W}) (31) functioned as effectively as the WT PPARγ in repressing the Nur77 protein level (*SI Appendix*, Fig. S5*H*), excluding the transcriptional regulation of Nur77 by PPARγ. Therefore, PPARγ acts as an upstream regulator to down-regulate the Nur77 protein level.

PPARγ influence on the protein stability of Nur77 was further supported by other evidence. Knockdown of PPARγ obviously mitigated the endogenous degradation of Nur77 (Fig. 5 *C*, *Upper*) in a close correlation to the suppressed ubiquitination level of endogenous Nur77 (Fig. 5*D*). When the ubiquitination site at residue Lys536 in Nur77 were mutated (from Lys to Arg) (32), PPARγ lost its influence on the ubiquitination and protein stability of Nur77 (Fig. 5 *C*, *Lower*, and Fig. 5*E*), while both Nur77 and Nur77^{K536R} were of comparable interactions with PPARγ (*SI Appendix*, Fig. S5*I*). Therefore, PPARγ influences the Nur77 stability by inducing the ubiquitination of Nur77 at Lys536. It was reported that Trim13, an E3 ubiquitin ligase, mediated the ubiquitination of Nur77 (33). Knockdown of PPARγ blocked while transfection of PPARγ enhanced the endogenous Trim13–Nur77 interaction (Fig. 5*F*), so PPARγ played a role in the Trim13–Nur77 interaction. When Trim13 was knocked down, PPARγ lost its influence on the ubiquitination of endogenous Nur77 (Fig. 5*G*). As a consequence, knockdown of Trim13 blocked the PPARγ-associated Nur77 degradation with the suppression of protein expression of CD36 and FABP4 (Fig. 5*H*) without impairing the endogenous Nur77–PPARγ interaction (*SI Appendix*, Fig. S5*J*). Since PPARγ also interacted with Trim13 (*SI Appendix*, Fig. S5*K*), these results suggest that PPARγ recruits Trim13 to degrade Nur77.

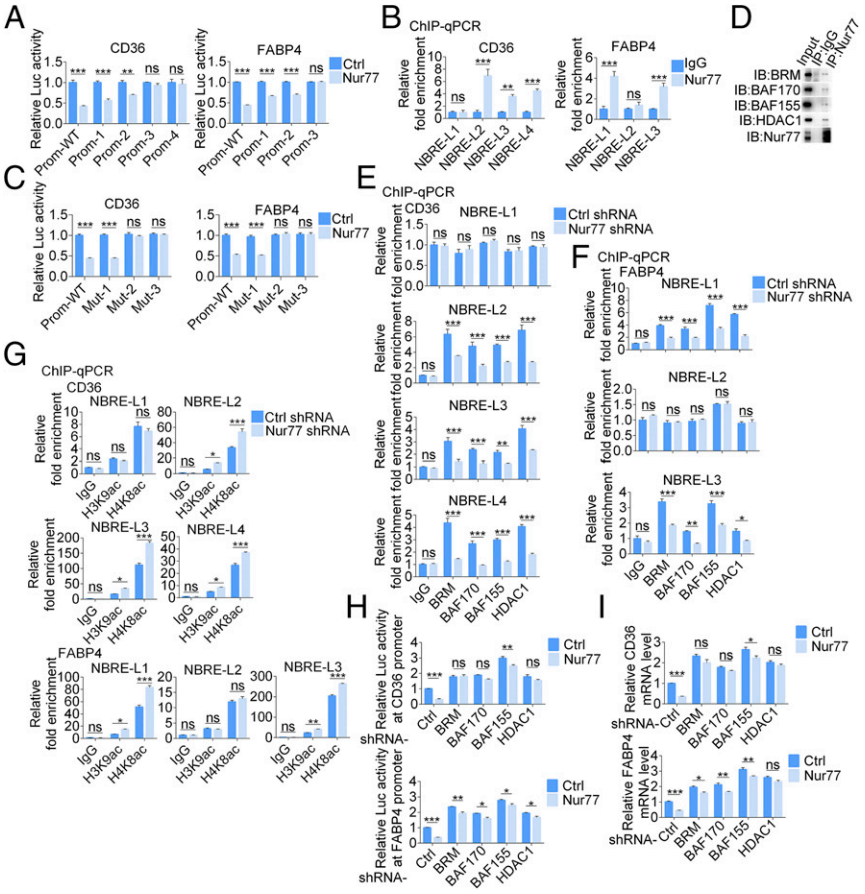

Fig. 4. Nur77 recruits corepressors to inhibit gene expression of CD36 and FABP4. (*A* and *C*) Effect of Nur77 on transcription activities of different truncations (*A*) and mutations (*C*) of CD36 and FABP4 promoters, detected by luciferase assay. (*B*) The occupations of Nur77 on the different NBRE-L sequences in the promoters of CD36 and FABP4, detected by ChIP-qPCR assay. (*D*) The interaction of Nur77 with different corepressors, detected by Co-IP assay. (*E* and *F*) The occupations of different corepressors on the different NBRE-L sequences in the promoters of CD36 (*E*) and FABP4 (*F*) in control or Nur77 knockdown MCF-7 cells, detected by ChIP-qPCR assay. (*G*) Histone acetylation levels at the NBRE-L sequences in the promoters of CD36 (*Upper*) and FABP4 (*Lower*) in control or Nur77 knockdown MCF-7 cells, detected by ChIP-qPCR assay. (*H* and *I*) Effects of different corepressors on Nur77-inhibited promoter activities (*H*) and gene-expression levels (*I*) of CD36 and FABP4. Different corepressors were first knocked down, and then Nur77 was transfected into MCF-7 cells. All data, except *D*, are presented as the mean ± SEM of two or three independent experiments. $*P < 0.05$, $**P < 0.01$, $***P < 0.001$, ns: not significant.

Domain mapping showed that the DNA binding domain (DBD) of PPARγ was responsible for the Nur77 binding (*SI Appendix*, Fig. S5*L*). Transfection of PPARγ ΔDBD lost its ability to strengthen endogenous interaction between Trim13 and Nur77 (Fig. 5*I*) and to mediate the endogenous Nur77 ubiquitination (Fig. 5*J*) and degradation (Fig. 5*K*) as compared to transfection of PPARγ, even though it could still interact with Trim13 (*SI Appendix*, Fig. S5*K*). The possibility of Trim13-induced PPARγ ubiquitination could be excluded as overexpression or knockdown of Trim13 did not impair the PPARγ expression levels (*SI Appendix*, Fig. S5*M*) and ubiquitination (*SI Appendix*, Fig. S5*N*). Taking these data together, it can be concluded that the PPARγ interaction with Nur77 is critical for the PPARγ-induced Nur77 degradation, which in turn leads to elevated levels of CD36 and FABP4 in breast cancer cells.

Csn-B Augments Nur77 Function by Impeding the PPARγ–Nur77 Interaction. The mechanism of PPARγ-mediated Nur77 degradation implies that an interference on the PPARγ–Nur77 interaction could enhance Nur77 stability to inhibit fatty acid uptake and cell proliferation during breast cancer progression. To this end, the Bodipy detection was employed to screen compounds from an in-house chemical library, by which octaketide cytosporone B (Csn-B) was identified as a candidate to inhibit fatty acid uptake in a Nur77-dependent manner (Fig. 6 *A* and *B*). Csn-B is known as an effective and specific Nur77 agonist (22). By attenuating the promoter activity and gene expression of CD36 and FABP4 (Fig. 6*C*), Csn-B markedly restrained lipid droplets accumulation in MCF-7 cells (Fig. 6*D*) to dampen the cell proliferation (Fig. 6*E*) in a Nur77-dependent manner. Similarly, Csn-B could inhibit fatty acid uptake (Fig. 6*F*) and consequent cell proliferation (Fig. 6*G*) in the primary tumor cells from PyMT-WT but not PyMT-KO mice. Hence, Csn-B is capable to potentiate the inhibitory effect of Nur77 in breast cancer cells.

Csn-B has been known to directly bind to the ligand binding domain (LBD) of Nur77 (22). It is notable that PPARγ also interacted with Nur77 LBD (*SI Appendix*, Fig. S6*A*). Treatment of Csn-B did not alter the transcription activity (*SI Appendix*, Fig. S6*B*) and expression of PPARγ (*SI Appendix*, Fig. S6*C*) in MCF-7 cells, but obviously interfered with the interaction between PPARγ and Nur77 in the endogenous case (Fig. 6*H*), and attenuated the PPARγ-induced ubiquitination of endogenous Nur77, as expected (Fig. 6*I*), thereby leading to the higher protein level of Nur77 (Fig. 6*J*). As a consequence, Csn-B suppressed the Nur77-mediated protein expression of CD36 and FABP4 (Fig. 6*K*). These Csn-B functions were mediated only by Nur77 but not two other members, Nurr1 and NOR1 in the NR4A nuclear receptor family, as Csn-B could not influence the transcriptional activity of Nurr1 and NOR1 (*SI Appendix*, Fig. S6*D*), in agreement with our previous report (22). Moreover, knockdown of neither Nurr1 nor NOR1 showed any effects on Csn-B's down-regulation of CD36/FABP4 expression and fatty acid uptake (*SI Appendix*, Fig. S6 *E* and *F*). These results demonstrate that Csn-B is an effective reagent to specifically stimulate Nur77 function in breast cancer cells through interfering with the PPARγ–Nur77 interaction and the PPARγ-mediated Nur77 degradation.

Complex Structure and Function of Csn-B with Nur77 LBD. The complex between Nur77 LBD and Csn-B was made by soaking the crystalline protein with the compound. It was revealed that Csn-B bound across two copies of LBD (Mol I and Mol II) in the asymmetric unit of the crystal (Fig. 7*A* and *SI Appendix*, Fig. S7*A*). This is a unique binding site, distinct from the previous binding positions for compounds, such as TMPA, THPN, and PDNPA

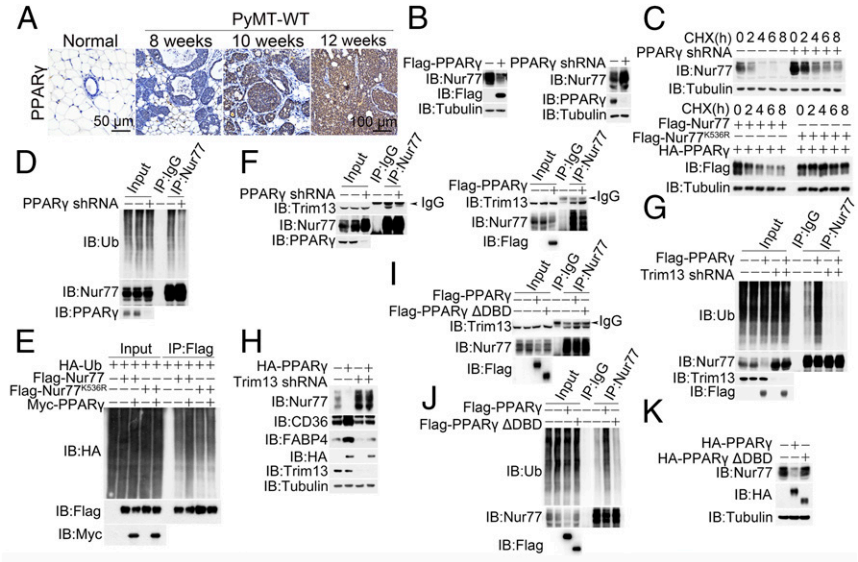

Fig. 5. PPARγ induces Nur77 degradation through ubiquitination pathway. (*A*) The level of PPARγ in mammary tumor samples of PyMT mice detected by IHC. Samples were the same as those in Fig. 1*B*. (*B*) Endogenous Nur77 expression levels in control, PPARγ transfection (*Left*) or knockdown (*Right*) MCF-7 cells. (*C*) The stability of Nur77 detected in the endogenous (*Upper*) or transfection case (*Lower*). MCF-7 cells were transfected with different plasmids and treated with CHX (100 μg/mL) at indicated times. (*D*) The ubiquitination of endogenous Nur77 in control or PPARγ knockdown MCF-7 cells. (*E*) Comparison of PPARγ effect on the ubiquitination of Nur77 and Nur77^{K536R}. Different plasmids as indicated were transfected into MCF-7 cells. (*F*) Effect of PPARγ on the endogenous Nur77–Trim13 interaction, determined in PPARγ knockdown (*Left*) or overexpressing (*Right*) MCF-7 cells. (*G* and *H*) Effect of Trim13 on PPARγ-induced endogenous Nur77 ubiquitination (*G*) and CD36 and FABP4 expression levels (*H*). Trim13 was knocked down first, and PPARγ were transfected into MCF-7 cells. (*I*–*K*) Effects of PPARγ ΔDBD on Nur77–Trim13 interaction (*I*), Nur77 ubiquitination (*J*), and endogenous Nur77 expression level (*K*) in MCF-7 cells. PPARγ was used as a positive control. Tubulin was used to determine the loading of total proteins.

(34–36). Co-IP experiments indicated that HA-PPARγ could outcompete dimeric Flag-Nur77 interaction to interact with monomeric Myc-Nur77. However, once Csn-B was added, the heterodimeric interaction between HA-PPARγ and Flag-Nur77 was hampered but the dimeric interaction between Flag-Nur77 and Myc-Nur77 were strengthened (Fig. 7*B*). Consistently, Csn-B greatly enhanced the formation of Nur77 homodimer, detected by cross-linking assay in the endogenous case (Fig. 7*C*). Since PPARγ DBD directly interacted with Nur77 LBD (*SI Appendix*, Fig. S7*B*), it seems that the role of Csn-B binding across the two monomeric LBD is to strengthen the Nur77 dimer formation, which would in turn result in a steric hindrance to block PPARγ binding, as supported by the docking model (Fig. 7*D*).

To support the role of Csn-B, the critical Nur77 residues for Csn-B binding were mutated for analysis. LBD residues D481, Q571, and R572 involved in the interactions with the compound in the complex structure, and the structure of Nur77 LBD$^{D481A/Q571A/R572W}$ suggested that the bulkier residues would preclude the Csn-B binding sterically in addition to abolishing the hydrogen bonding (Fig. 7*E*). Both fluorescence quenching and thermal-shift assays consistently indicated that this triple mutant of Nur77 LBD lost most of its ability to bind Csn-B (Fig. 7 *F* and *G* and *SI Appendix*, Fig. S7*C*). As a result, Csn-B not only failed to activate the transcriptional activity of Nur77$^{D481A/Q571A/R572W}$ (*SI Appendix*, Fig. S7*D*), but also lost the capacity to facilitate the formation of dimeric LBD$^{D481A/Q571A/R572W}$ (Fig. 7*H*). In contrast, the interaction of the Nur77$^{D481A/Q571A/R572W}$ mutant with PPARγ was not impaired in the presence of Csn-B, in the transfection experiments (Fig. 7*I*) or the in vitro pull-down assays (*SI Appendix*, Fig. S7*E*). It can also be shown that a reintroduction of Nur77$^{D481A/Q571A/R572W}$ did not compensate for the role of Nur77-WT in Csn-B-inducing inhibition of fatty acid uptake in Nur77-knocked down MCF-7 cells, even in the presence of lipid mixture (Fig. 7*J*). These data supplement favorably for the finding that Csn-B binding strengthens LBD's dimeric interaction to outcompete the PPARγ binding, and the binding of Csn-B with Nur77 is a prerequisite for the inhibitory function of Csn-B in breast cancer cells.

Csn-B Effectively Inhibits Breast Cancer Progression. The physiological potential of Csn-B in mouse models was also investigated. Csn-B treatment sufficiently retarded tumor initiation (Fig. 8*A*), caused a significant delay in tumor progression (*SI Appendix*, Fig. S8*A*) with reduced tumor sizes and weights in PyMT-WT mice but not in PyMT-KO mice (Fig. 8*B*). Similarly, Csn-B administration retarded tumor initiation and progression in MPA/DMBA-induced mammary tumor model made in WT mice but not KO mice (Fig. 8*C* and *SI Appendix*, Fig. S8*B*), which led to the decreased tumor sizes and weights in the same mice (Fig. 8*D*). In these two mouse models, Ki67 expression levels in tumor samples were down-regulated by Csn-B treatment in a Nur77-dependent manner (*SI Appendix*, Fig. S8*C*). Immunohistochemical (IHC) analysis revealed that Csn-B treatment significantly enhanced Nur77 protein levels either in the MMTV-PyMT or in the MPA/DMBA-induced mammary tumor samples (Fig. 8*E*) with significant attenuation of protein expressions of CD36 and FABP4 in mammary tumor tissues of WT but not KO mice (Fig. 8*F*). As a result, the accumulation of lipid droplets in tumor samples were substantially inhibited by Csn-B in PyMT-WT tumor sample (*SI Appendix*, Fig. S8*D*). Clearly, Csn-B effectively suppresses breast cancer progression through the Nur77 mediation.

It could also be demonstrated that the expressions of PPARγ, CD36, and FABP4 were significantly elevated either in clinical samples of breast cancer as compared to the corresponding para-tissues (Fig. 8*G* and Dataset S2) or in different developmental stages of the breast cancer (Fig. 8*H* and Dataset S2). In these clinical samples, the level of Nur77 was notably decreased, implicating a strong clinical correlation of Nur77 with PPARγ, CD36, and FABP4. Follow-up studies with these patients indicated that the patients with higher levels of Nur77 expression was closely associated with good clinical prognoses, while a higher level of PPARγ, CD36, or FABP4 expression was consistently linked to poor clinical prognoses (Fig. 8*I*). Together, all of these results demonstrate that Nur77 and PPARγ are potential biomarkers for the clinical outcome of breast cancer, and Csn-B is a promising lead compound to treat breast cancer by acting as an agonist of Nur77.

Discussion

Adipocytes, as an external lipid donor in the microenvironment of breast cancer tissues, are a major source of lipids to breast cancer cells through their direct communications. An interruption of this lipid uptake process would hamper cancer cell growth. However, there was a lack of either knowledge on or means for interfering with the molecular process of exogenous lipid uptake to arrest the growth of breast cancer cells. In this study, Nur77 was shown to be a key player in repressing breast

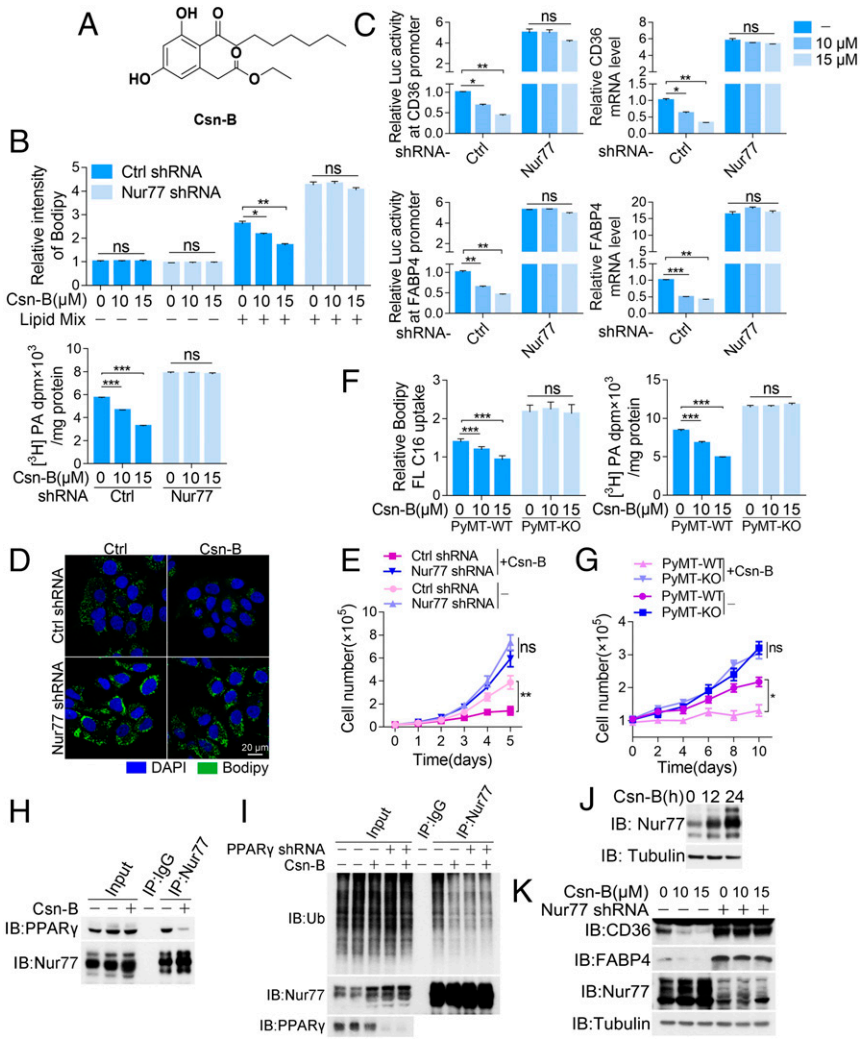

Fig. 6. Csn-B inhibits fatty acid uptake through blocking PPARγ–Nur77 interaction. Csn-B at indicated concentrations or 10 μM was used to treat MCF-7 cells for 24 h, unless specially defined. (*A*) Structure of Csn-B. (*B–E*) Effects of Csn-B on lipid accumulation (*B*, *Upper*), fatty acid uptake (*Lower*), transcriptional activity (*C*, *Left*) and mRNA levels (*Right*) of CD36 and FABP4, lipid content (*D*), and cell proliferation (*E*) in control or Nur77 knockdown MCF-7 cells. Cells were cultured with lipid mixture (*D* and *E*). (*F* and *G*) Effects of Csn-B on fatty acids uptake (*F*) and cell proliferation (*G*) in primary tumor cells from mammary tumors of PyMT mice. Cells were cultured with lipid mixture (*G*). (*H* and *I*) Effects of Csn-B on the endogenous PPARγ–Nur77 interaction (*H*) and PPARγ-induced endogenous Nur77 ubiquitination (*I*). PPARγ was knocked down in MCF-7 cells. (*J* and *K*) Effect of Csn-B on expression levels of endogenous Nur77 (*J*), CD36 and FABP4 (*K*). Tubulin was used to determine the loading of total proteins. Data are presented as the mean ± SEM of two or three independent experiments. $*P < 0.05$, $**P < 0.01$, $***P < 0.001$, ns: not significant.

cancer cells uptake of exogenous fatty acids through recruiting SWI/SNF complex and HDAC1 to transcriptionally repress CD36 and FABP4 expressions, leading to the inhibition of breast cancer development. Nevertheless, this role of Nur77 was nullified during breast cancer progression due to highly expressed nuclear receptor PPARγ that interacted with Nur77 to recruit ubiquitin ligase Trim13 to target Nur77 for degradation. Subsequently, we identified Csn-B from an in-house chemical library as an effective and specific lead compound to treat breast cancer through disrupting the Nur77–PPARγ association, which enhanced the Nur77's blockage of the fatty acid uptake from tumor's metabolic microenvironment (Fig. 8*J*). Together, the data in this study engender a better understanding on the inhibitory function of Nur77 in breast cancer through metabolic reprogramming of lipids.

As a major component in the breast cancer stroma, adipocytes are capable of secreting large quantities of metabolic substrates, such as fatty acids, to establish a metabolic tumor microenvironment (8, 37). This altered metabolic microenvironment facilitates the adaptation of breast cancer cells to the easy availability of metabolic substrates, leading to the extracellular lipid addiction of breast cancer. We found that the proliferation of breast cancer cells largely relied on the coculture of adipocytes or the addition of exogenous lipid mixture. Therefore, breast cancer cells are able to adapt to their metabolic microenvironment in a flexible manner to take up "ready-made" lipids from the surrounding environment to bypass the de novo lipid synthesis. In this regard, targeting the uptake of extracellular lipid could be a promising approach for breast cancer therapy.

The uptake of the majority of fatty acids in cells depends on several transmembrane proteins and cytoplasmic fatty acid binding proteins, such as CD36 and FABP4. These proteins provide a regulatory platform for cells to fine-tune the availability of fatty acids to meet the metabolic demand. Nur77, as a negative regulator for fatty acid uptake in breast cancer, could directly bind to NBRE-L sequences in the promoters of CD36 and FABP4 for the recruitment of the SWI/SNF complex and HDAC1 to repress their expressions, leading to the restrained fatty acid uptake and inhibited breast cancer progression both in vitro and in vivo. The SWI/SNF complex plays an important role in the regulation of fatty acid oxidation (38). The present study further extended its functions to fatty acid uptake, implicating a multifunctional attribute to the SWI/SNF complex in lipid metabolism. The inhibition of CD36 or FABP4 by Nur77 was also reported in macrophages (39) and adipocytes of mice (40), although their detailed regulatory mechanisms were not demonstrated. It may therefore suggest a common Nur77 role in regulating lipid uptake in different tissues.

The regulation of Nur77 on fatty acid uptake can be counteracted by PPARγ, which was generally highly expressed in breast cancer (41). PPARγ regulated the level of Nur77 in a manner independent of its transcriptional activity by recruiting

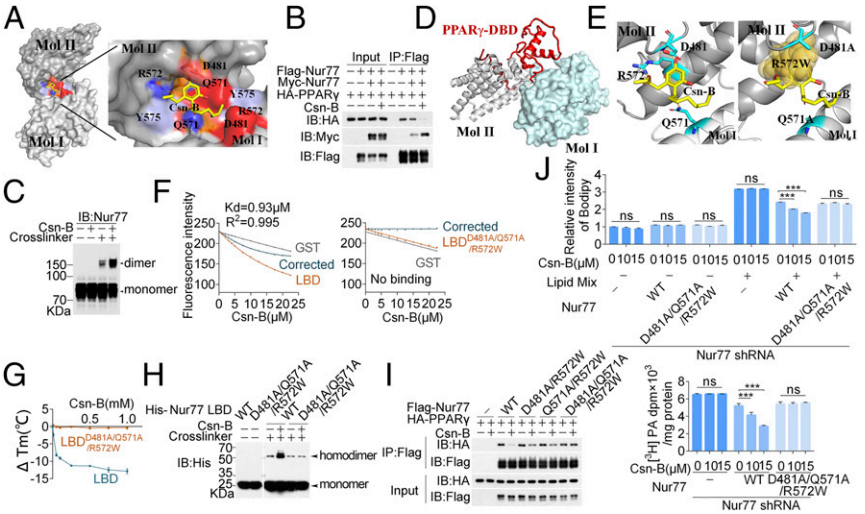

Fig. 7. Csn-B functions by binding at the Nur77 dimer interface. (*A*) Csn-B bridges the two LBDs. The two Nur77 monomers, Mol I and Mol II, are with different conformations at the crystallographic asymmetric unit. The Nur77 residues involved in the interaction are labeled and surface changes around the binding site are colored in red for negative charges and in blue for positive charges. (*B*) Effects of Csn-B on the interaction of the Nur77–Nur77 homodimer and Nur77–PPARγ heterodimer. Plasmids of Nur77 with different tags and PPARγ were transfected into MCF-7 cells. (*C*) Csn-B promoted endogenous Nur77 dimerization in MCF-7 cells, detected by the cross-linking reactions. (*D*) Molecular docking shows the preferential PPARγ DBD (red) interaction with LBD Molecule I (cyan). The place of Mol II (gray) would be clash with PPARγ DBD, indicating that the formations of LBD homodimer and Nur77–PPARγ heterodimer are mutually exclusive. (*E*) Critical Nur77 residues for Csn-B binding. Residues D481, Q571, and R572 are at the Csn-B binding site (*Left*). Mutation of D481A and Q571A abolished hydrogen bonds between Csn-B and Nur77 while R572W (spheres in yellow) produced space constraints for Csn-B binding (*Right*). (*F* and *G*) Csn-B binds to Nur77 LBD (*F*, *Left*) but not LBD mutant (*F*, *Right*). Fluorescence spectra of His-LBD or LBD mutant was obtained in the absence or presence of increasing amounts of Csn-B. GST was used as inner filter controls (*F*). The ΔTm value of Csn-B binding to Nur77 LBD and LBD mutant with different Csn-B concentrations (0 to 1 mM) in a thermal-shift assay (*G*). (*H*) Effect of Csn-B on the Nur77 LBD dimerization. The in vitro cross-linking reactions were performed. (*I* and *J*) Effects of Csn-B on the interaction of PPARγ–Nur77 mutant (*I*), lipid droplet accumulation, and fatty acid uptake (*J*) in MCF-7 cells. Nur77 was knocked down first, and the siRNA-resistant form of Nur77 or Nur77 mutant was reintroduced into the cells. Cells were cultured in the medium with or with lipid mixture addition. Data are presented as the mean ± SEM of two or three independent experiments. ***$P < 0.001$, ns: not significant.

the E3 ligase Trim13 to ubiquitinate Nur77 for the proteasomal degradation and subsequent up-regulation of CD36 and FABP4 expressions. Since PPARγ was also reported as a transcriptional activator for multiple genes involved in lipid metabolism, including CD36 and FABP4 (42, 43), it regulates the fatty acid uptake through both transcriptional-dependent and -independent pathways. Due to the diversity and complexity of the downstream genes, targeting the transcriptional activity of PPARγ did not produce a consistent outcome on the development of breast cancer (44, 45). This interference on the PPARγ–Nur77 interplay may represent a more focus strategy to screen compounds for breast cancer intervention.

Despite the fact that no physiological ligand for Nur77 has been identified up to date, several small molecular compounds, such as Csn-B (22) and bis-indole–derived compounds (46, 47), were identified as the agonists for Nur77, and their antitumor functions in gastric and colorectal cancer have also been reported (14, 48). In the present study, Csn-B inhibited breast cancer by disrupting the association between Nur77 and PPARγ. Structural and mutational analysis indicated that the binding of Csn-B with Nur77 is a prerequisite for the Nur77 inhibitory effect. Enhancing the Nur77–Nur77 homodimeric interaction by Csn-B establishes a steric hindrance to impede the formation of the Nur77–PPARγ heterodimer, indicating that Nur77–Nur77 and Nur77–PPARγ interactions are mutually exclusive. In addition, this Csn-B–induced Nur77 dimer formation may also bolster the role of Csn-B to function as an agonist to stimulate the transcriptional activity of Nur77, since the Nur77 dimer is more effective in transcriptional activation (22). Thus, Csn-B modulates multiple Nur77 functions transcriptionally as well as posttranscriptionally.

The involvement of Nur77 in breast cancer has been reported but remains contradictory. On the one hand, Nur77 functions as a tumor suppressor to inhibit the proliferation and migration of breast cancer cells (16, 17). Hence, Nur77 is thought to be a favorable prognosis factor in patients with triple-negative breast cancer or in a large cohort of breast cancer patients (16, 18). On the other hand, inflammation-induced Nur77 promotes invasion and metastasis of breast cancer cells in a TGF-β–dependent or β1-integrin–dependent manner (19–21), which suggests a pro-oncogenic role of Nur77 in breast cancer. This discrepancy is reconciled by the notion that the distinct functions of Nur77 in breast cancer may depend on different stimuli and breast cancer subtypes. In fact, the context-dependent functions of Nur77 have also been demonstrated in other cancers, such as colorectal cancers (14, 49). Therefore, dissecting the functions of Nur77 in breast cancer using different mouse models could provide a more comprehensive insight into the in vivo role of Nur77 on tumor development.

Experimental Procedures

Mammary Tumor Cell Isolation. For primary mammary tumor cells, spontaneous mammary tumors were removed from PyMT-WT or PyMT-KO female mice, minced, and incubated with digestion solution (containing 5% FBS, 10 ng/mL epidermal growth factor, 500 ng/mL hydrocortisone, 5 μg/mL insulin, 20 ng/mL cholera toxin, 300 U/mL collagenase type I and 100 U/mL hyaluronidase) at 37 °C for 3 h. The digested cell clumps were pelleted by centrifugation, resuspended in 0.25% trypsin-EDTA solution at 37 °C for 2 min, and then subjected to 5 mg/mL dispase and 0.1 mg/mL DNase digestion for another 5 min. Erythrocytes were removed by using red blood cell lysis buffer, and the cell suspensions were filtered through a 100-μm cell strainer. The single cell suspensions were collected and maintained in DMEM containing 10% FBS.

All animals were maintained at Laboratory Animal Center in Xiamen University (China) in accordance with the institutional guidelines. All animal experiments were approved by the Animal Ethics Committee of Xiamen University (acceptance no. XMULAC20120030).

Immunofluorescence for Lipid. For natural lipid staining, cells seeded on microscope cover glasses were fixed with 4% paraformaldehyde, and incubated with 1 ng/mL Bodipy 493/503 for 20 min at room temperature. The cells were stained with DAPI before mounting and imaging on LSM 780 microscope (Zeiss).

For tissue immunofluorescence, frozen sections were incubated with anti-Ki67 antibody (1:50) overnight at 4 °C in a humidified chamber. The sections were then washed with PBS and incubated with Alexfluor 594-conjugated secondary antibody (Life Technologies) for 1 h at room temperature, and then incubated with 1 ng/mL Bodipy 493/503 for 20 min at room temperature. The sections were stained with DAPI before mounting and imaging.

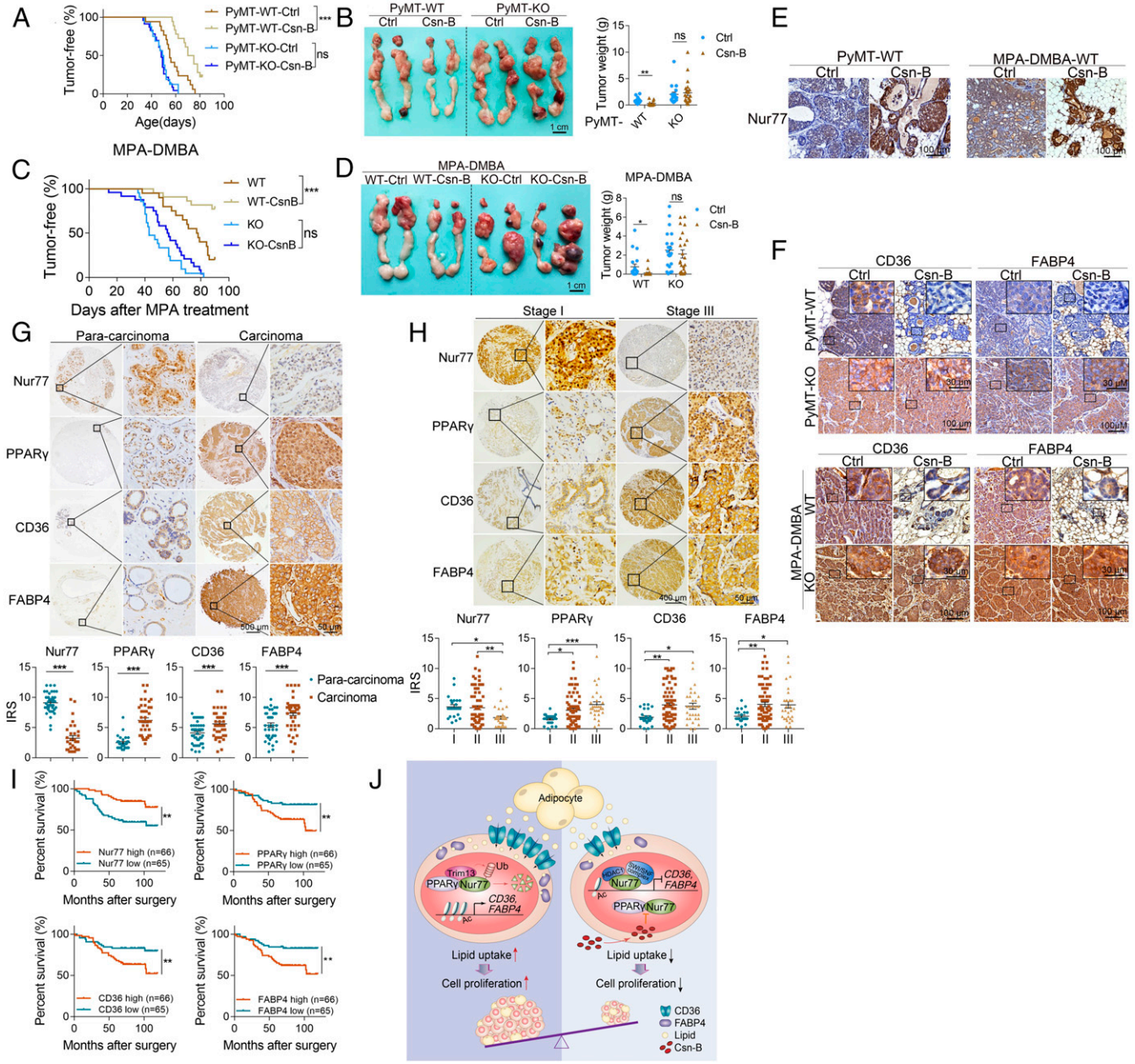

Fig. 8. Roles of Csn-B in repression of breast cancer progression. (*A*–*D*) Effects of intravenous injection of Csn-B (10 mg/kg) on mammary tumor development in PyMT (*A* and *B*, female, 12 wk, $n = 17$ for WT, $n = 17$ for KO, $n = 18$ for WT-Csn-B, and $n = 20$ for KO-Csn-B) or MPA/DMPA mammary tumor models (*C* and *D*, female, 13 wk, $n = 20$ for WT, $n = 21$ for KO, $n = 22$ for WT-Csn-B, and $n = 24$ for KO-Csn-B). (*E* and *F*) Effects of Csn-B on the expression of Nur77 (*E*), CD36 and FABP4 (*F*) in mammary tumor tissues of PyMT or MPA/DMPA mouse models. Samples were from above. (*G* and *H*) Comparison of expression levels of Nur77 ($n = 71$), PPARγ ($n = 72$), CD36 ($n = 87$), and FABP4 ($n = 83$) between clinical carcinoma samples and their paired paracarcinoma samples (*G*), or different stages of clinical breast cancer samples (*H*, $n = 23$ for stage I, $n = 75$ for stage II, $n = 30$ for stage III). (*I*) Kaplan–Meier survival curve shows correlation between overall survival of breast cancer patients and Nur77, PPARγ, CD36, or FABP4 expression levels, respectively. Patients were classified into two group based on the median of the expression value of those genes in the entire population of patients, as defined in *SI Appendix, Supplemental Materials and Methods*. (*J*) A working model for this study. Data are presented as the mean ± SEM $^*P < 0.05$, $^{**}P < 0.01$, $^{***}P < 0.001$, ns: not significant.

Tissue Microarray, Histology, and IHC Assays. A breast cancer tissue microarray (TMAs; HBreDuc140Sur02 and HBreD090CS01) with patient diagnosis data were purchased from Shanghai Outdo Biotech Company. For histological analysis, H&E staining was carried out according to the manufacturer's standard procedures.

IHC staining of mouse mammary tissue sections and TMAs was performed using UltraSensitiveTM SP (Mouse/Rabbit) IHC Kit (Maxim Biotechnologies, Fujian, China; KIT-9710). The mouse tissue sections were stained with anti-Nur77 (1:100), anti-PPARγ (1:100), anti-CD36 (1:400), anti-FABP4 (1:200), or anti-Ki67 (1:150) primary antibodies, and the TMAs were stained with anti-Nur77 (1:200), anti-PPARγ (1:100), anti-CD36 (1:200), or anti-FABP4 (1:200) primary antibodies, and then followed by successively incubating with biotin-labeled anti-mouse/rabbit IgG and peroxidase-conjugated streptavidin. The stained samples were visualized by using DAB Detection Kit (Maxim Biotechnologies, Kit-0014). The IHC results are quantified using immuoreactive score system (50). Each sample was subjected to blind evaluation by three people and the mean score was considered as the final immuoreactive score.

Statistical Analysis. The error bars are represented as the mean ± SEM. The statistical analysis of the difference between two groups was carried out by

using the two-tailed Student's *t* test and multiple group comparisons were determined using one-way or two-way ANOVA followed by Tukey's post hoc test. Survival curves were derived by the Kaplan–Meier method and compared by log-rank test. The significance thresholds were defined as statistically significant (*$P < 0.05$), highly significant (**$P < 0.01$), or extremely significant (***$P < 0.001$); ns, not significant. The statistical analysis was performed using GraphPad Prism 6.

Data Availability. The structure factors and atomic coordinates for CsnB-bound NUR77 LBD have been deposited in the Protein Data Bank, http://www.wwpdb.org/ (PDB ID code 6KZ5). The RNA-seq data have been deposited in the Gene Expression Omnibus database, https://www.ncbi.nlm.nih.gov/geo (accession no. GSE131895). Source data for *SI Appendix*, Fig. S4*B* have been provided as Dataset S1. Statistical source data supporting Fig. 8 *G* and *H* are provided in Dataset S2. All other data that support the findings of this study are included in the main text or *SI Appendix*.

ACKNOWLEDGMENTS. We thank the Dr. Da-lin Shi group, including You-ting Ye, Li-zhen Lin (School of The Environment & Ecology, Xiamen University), for kindly providing technological assistance with detection of [9,10-3H] palmitate acid and data analysis; Yaying Wu, Zheni Xu, and Dr. Changchuan Xie (School of Life Sciences, Xiamen University) for mass spectrometry experiments and data analysis; and Dr. Hong-rui Wang (School of Life Sciences, Xiamen University) for kindly providing the HA-Ub plasmid. The crystallographic data collection at Beamline BL19U1 at Shanghai Synchrotron Radiation Facility is gratefully acknowledged. This study was supported by the National Natural Science Foundation of China (91853203, U1905206, 81730070, 31822013, 81672695), State Bureau of Foreign Experts and Ministry of Education of China (BP2018017), and the Fundamental Research Funds for the Central Universities of China (20720190083).

1. F. Bray *et al*., Global cancer statistics 2018: GLOBOCAN estimates of incidence and mortality worldwide for 36 cancers in 185 countries. *CA Cancer J. Clin.* **68**, 394–424 (2018).
2. M. Morrow, S. J. Schnitt, L. Norton, Current management of lesions associated with an increased risk of breast cancer. *Nat. Rev. Clin. Oncol.* **12**, 227–238 (2015).
3. G. van Meer, D. R. Voelker, G. W. Feigenson, Membrane lipids: Where they are and how they behave. *Nat. Rev. Mol. Cell Biol.* **9**, 112–124 (2008).
4. J. A. Menendez, R. Lupu, Fatty acid synthase and the lipogenic phenotype in cancer pathogenesis. *Nat. Rev. Cancer* **7**, 763–777 (2007).
5. V. Chajès, M. Cambot, K. Moreau, G. M. Lenoir, V. Joulin, Acetyl-CoA carboxylase α is essential to breast cancer cell survival. *Cancer Res.* **66**, 5287–5294 (2006).
6. K. S. Lucenay *et al*., Cyclin E associates with the lipogenic enzyme ATP-citrate lyase to enable malignant growth of breast cancer cells. *Cancer Res.* **76**, 2406–2418 (2016).
7. S. Balaban *et al*., Adipocyte lipolysis links obesity to breast cancer growth: Adipocyte-derived fatty acids drive breast cancer cell proliferation and migration. *Cancer Metab.* **5**, 1 (2017).
8. C. Blücher, S. C. Stadler, Obesity and breast cancer: Current insights on the role of fatty acids and lipid metabolism in promoting breast cancer growth and progression. *Front. Endocrinol. (Lausanne)* **8**, 293 (2017).
9. B. Dirat *et al*., Cancer-associated adipocytes exhibit an activated phenotype and contribute to breast cancer invasion. *Cancer Res.* **71**, 2455–2465 (2011).
10. K. M. Nieman *et al*., Adipocytes promote ovarian cancer metastasis and provide energy for rapid tumor growth. *Nat. Med.* **17**, 1498–1503 (2011).
11. T. G. Hazel, D. Nathans, L. F. Lau, A gene inducible by serum growth factors encodes a member of the steroid and thyroid hormone receptor superfamily. *Proc. Natl. Acad. Sci. U.S.A.* **85**, 8444–8448 (1988).
12. X. X. Li *et al*., Nuclear receptor Nur77 facilitates melanoma cell survival under metabolic stress by protecting fatty acid oxidation. *Mol. Cell* **69**, 480–492.e7 (2018).
13. X. L. Bian *et al*., Nur77 suppresses hepatocellular carcinoma via switching glucose metabolism toward gluconeogenesis through attenuating phosphoenolpyruvate carboxykinase sumoylation. *Nat. Commun.* **8**, 14420 (2017).
14. H.-Z. Chen *et al*., The orphan receptor TR3 suppresses intestinal tumorigenesis in mice by downregulating Wnt signalling. *Gut* **61**, 714–724 (2012).
15. S. E. Mullican *et al*., Abrogation of nuclear receptors Nr4a3 and Nr4a1 leads to development of acute myeloid leukemia. *Nat. Med.* **13**, 730–735 (2007).
16. H. Wu *et al*., Nuclear receptor NR4A1 is a tumor suppressor down-regulated in triple-negative breast cancer. *Oncotarget* **8**, 54364–54377 (2017).
17. A. N. Alexopoulou *et al*., Dissecting the transcriptional networks underlying breast cancer: NR4A1 reduces the migration of normal and breast cancer cell lines. *Breast Cancer Res.* **12**, R51 (2010).
18. C. Zhong, Y. Mai, H. Gao, W. Zhou, D. Zhou, Mitochondrial targeting of TR3 is involved in TPA induced apoptosis in breast cancer cells. *Gene* **693**, 61–68 (2019).
19. E. Hedrick, S. Safe, Transforming growth factor β/NR4A1-Inducible breast cancer cell migration and epithelial-to-mesenchymal transition is p38α (mitogen-activated protein kinase 14) dependent. *Mol. Cell. Biol.* **37**, e00306–e00317 (2017).
20. E. Hedrick, S.-O. Lee, R. Doddapaneni, M. Singh, S. Safe, NR4A1 antagonists inhibit β1-integrin-dependent breast cancer cell migration. *Mol. Cell. Biol.* **36**, 1383–1394 (2016).
21. F. Zhou *et al*., Nuclear receptor NR4A1 promotes breast cancer invasion and metastasis by activating TGF-β signalling. *Nat. Commun.* **5**, 3388 (2014).
22. Y. Zhan *et al*., Cytosporone B is an agonist for nuclear orphan receptor Nur77. *Nat. Chem. Biol.* **4**, 548–556 (2008).
23. E. Y. Lin *et al*., Progression to malignancy in the polyoma middle T oncoprotein mouse breast cancer model provides a reliable model for human diseases. *Am. J. Pathol.* **163**, 2113–2126 (2003).
24. Y. Yin *et al*., Characterization of medroxyprogesterone and DMBA-induced multilineage mammary tumors by gene expression profiling. *Mol. Carcinog.* **44**, 42–50 (2005).
25. I. J. Goldberg, R. H. Eckel, N. A. Abumrad, Regulation of fatty acid uptake into tissues: Lipoprotein lipase- and CD36-mediated pathways. *J. Lipid Res.* **50** (suppl.), S86–S90 (2009).
26. J. Storch, A. E. A. Thumser, The fatty acid transport function of fatty acid-binding proteins. *Biochim. Biophys. Acta* **1486**, 28–44 (2000).
27. K. Palumbo-Zerr *et al*., Orphan nuclear receptor NR4A1 regulates transforming growth factor-β signaling and fibrosis. *Nat. Med.* **21**, 150–158 (2015).
28. M. Ahmadian *et al*., PPARγ signaling and metabolism: The good, the bad and the future. *Nat. Med.* **19**, 557–566 (2013).
29. M. K. Sakharkar *et al*., Therapeutic implications of targeting energy metabolism in breast cancer. *PPAR Res.* **2013**, 109285 (2013).
30. M. Bionaz, B. J. Thering, J. J. Loor, Fine metabolic regulation in ruminants via nutrient-gene interactions: Saturated long-chain fatty acids increase expression of genes involved in lipid metabolism and immune response partly through PPAR-α activation. *Br. J. Nutr.* **107**, 179–191 (2012).
31. M. Agostini *et al*., Non-DNA binding, dominant-negative, human PPARgamma mutations cause lipodystrophic insulin resistance. *Cell Metab.* **4**, 303–311 (2006).
32. M. Hu *et al*., Celastrol-induced Nur77 interaction with TRAF2 alleviates inflammation by promoting mitochondrial ubiquitination and autophagy. *Mol. Cell* **66**, 141–153.e6 (2017).
33. B. Huang, H. Z. Pei, H.-W. Chang, S.-H. Baek, The E3 ubiquitin ligase Trim13 regulates Nur77 stability via casein kinase 2α. *Sci. Rep.* **8**, 13895 (2018).
34. L. Li *et al*., Impeding the interaction between Nur77 and p38 reduces LPS-induced inflammation. *Nat. Chem. Biol.* **11**, 339–346 (2015).
35. W. J. Wang *et al*., Orphan nuclear receptor TR3 acts in autophagic cell death via mitochondrial signaling pathway. *Nat. Chem. Biol.* **10**, 133–140 (2014).
36. Y. Y. Zhan *et al*., The orphan nuclear receptor Nur77 regulates LKB1 localization and activates AMPK. *Nat. Chem. Biol.* **8**, 897–904 (2012).
37. A. J. Hoy, S. Balaban, D. N. Saunders, Adipocyte-tumor cell metabolic crosstalk in breast cancer. *Trends Mol. Med.* **23**, 381–392 (2017).
38. Y. L. Deribe *et al*., Author correction: Mutations in the SWI/SNF complex induce a targetable dependence on oxidative phosphorylation in lung cancer. *Nat. Med.* **24**, 1627 (2018).
39. P. I. Bonta *et al*., Nuclear receptors Nur77, Nurr1, and NOR-1 expressed in atherosclerotic lesion macrophages reduce lipid loading and inflammatory responses. *Arterioscler. Thromb. Vasc. Biol.* **26**, 2288–2294 (2006).
40. K. Duszka *et al*., Nr4a1 is required for fasting-induced down-regulation of Pparγ2 in white adipose tissue. *Mol. Endocrinol.* **27**, 135–149 (2013).
41. I. Kotta-Loizou, C. Giaginis, S. Theocharis, The role of peroxisome proliferator-activated receptor-γ in breast cancer. *Anticancer. Agents Med. Chem.* **12**, 1025–1044 (2012).
42. M. Febbraio, D. P. Hajjar, R. L. Silverstein, CD36: A class B scavenger receptor involved in angiogenesis, atherosclerosis, inflammation, and lipid metabolism. *J. Clin. Invest.* **108**, 785–791 (2001).
43. D. B. Savage *et al*., Resistin/Fizz3 expression in relation to obesity and peroxisome proliferator-activated receptor-γ action in humans. *Diabetes* **50**, 2199–2202 (2001).
44. I. Kotta-Loizou, C. Giaginis, S. Theocharis, The role of peroxisome proliferator-activated receptor-γ in breast cancer. *Anti-Cancer Agents Med. Chem.* **12**, 1025–1044 (2012).
45. C. D. Allred, M. W. Kilgore, Selective activation of PPARgamma in breast, colon, and lung cancer cell lines. *Mol. Cell. Endocrinol.* **235**, 21–29 (2005).
46. S. Safe *et al*., Nuclear receptor 4A (NR4A) family—Orphans no more. *J. Steroid Biochem. Mol. Biol.* **157**, 48–60 (2016).
47. S. D. Cho *et al*., Nur77 agonists induce proapoptotic genes and responses in colon cancer cells through nuclear receptor-dependent and nuclear receptor-independent pathways. *Cancer Res.* **67**, 674–683 (2007).
48. J. J. Liu *et al*., A unique pharmacophore for activation of the nuclear orphan receptor Nur77 in vivo and in vitro. *Cancer Res.* **70**, 3628–3637 (2010).
49. H. Wu *et al*., Regulation of Nur77 expression by β-catenin and its mitogenic effect in colon cancer cells. *FASEB J.* **25**, 192–205 (2011).
50. N. Fedchenko, J. Reifenrath, Different approaches for interpretation and reporting of immunohistochemistry analysis results in the bone tissue—A review. *Diagn. Pathol.* **9**, 221 (2014).